Regular Article

IMMUNOBIOLOGY AND IMMUNOTHERAPY

Therapeutic activity of GARP:TGF-β1 blockade in murine primary myelofibrosis

Sara Lecomte,[1,*] Julien Devreux,[1,*] Grégoire de Streel,[1] Nicolas van Baren,[1] Violaine Havelange,[1,2] David Schröder,[1] Noora Vaherto,[1] Christophe Vanhaver,[1] Christophe Vanderaa,[1] Noémie Dupuis,[1] Christian Pecquet,[1,3] Pierre G. Coulie,[1,4] Stefan N. Constantinescu,[1,3-5] and Sophie Lucas[1,4]

[1]de Duve Institute, Université catholique de Louvain, Brussels, Belgium; [2]Department of Hematology, Cliniques universitaires Saint-Luc, Brussels, Belgium; [3]Ludwig Institute for Cancer Research Brussels, Brussels, Belgium; [4]Walloon Excellence in Life Sciences and Biotechnology, Wavre, Belgium; and [5]Nuffield Department of Medicine, Ludwig Institute for Cancer Research Oxford, University of Oxford, Oxford, United Kingdom

KEY POINTS

- **Anti-GARP:TGF-β1 mAb exerts antitumor activity in myeloproliferative neoplasms by selectively blocking Treg-derived TGF-β1.**

- **Targeting Treg functions is feasible and has immune-mediated therapeutic activity in blood cancers.**

Primary myelofibrosis (PMF) is a myeloproliferative neoplasm characterized by the clonal expansion of myeloid cells, notably megakaryocytes (MKs), and an aberrant cytokine production leading to bone marrow (BM) fibrosis and insufficiency. Current treatment options are limited. TGF-β1, a profibrotic and immunosuppressive cytokine, is involved in PMF pathogenesis. While all cell types secrete inactive, latent TGF-β1, only a few activate the cytokine via cell type–specific mechanisms. The cellular source of the active TGF-β1 implicated in PMF is not known. Transmembrane protein GARP binds and activates latent TGF-β1 on the surface of regulatory T lymphocytes (Tregs) and MKs or platelets. Here, we found an increased expression of GARP in the BM and spleen of mice with PMF and tested the therapeutic potential of a monoclonal antibody (mAb) that blocks TGF-β1 activation by GARP-expressing cells. GARP:TGF-β1 blockade reduced not only fibrosis but also the clonal expansion of transformed cells. Using mice carrying a genetic deletion of *Garp* in either Tregs or MKs, we found that the therapeutic effects of GARP:TGF-β1 blockade in PMF imply targeting GARP on Tregs. These therapeutic effects, accompanied by increased IFN-γ signals in the spleen, were lost upon CD8 T-cell depletion. Our results suggest that the selective blockade of TGF-β1 activation by GARP-expressing Tregs increases a CD8 T-cell-mediated immune reaction that limits transformed cell expansion, providing a novel approach that could be tested to treat patients with myeloproliferative neoplasms.

Introduction

Philadelphia-negative myeloproliferative neoplasms (MPNs) are hematopoietic stem cell (HSC) disorders characterized by the clonal expansion of differentiated myeloid cells. They encompass polycythemia vera, essential thrombocythemia and primary myelofibrosis (PMF). PMF bears the worst prognosis with a median overall survival of 4.4 years.[1] Characteristic features of PMF include abnormal proliferation of immature megakaryocytes (MKs) and aberrant production of proinflammatory cytokines, leading to progressive bone marrow (BM) fibrosis, BM failure, and extramedullary hematopoiesis. Transformation into acute myeloid leukemia can also arise and constitutes a major concern. The physiopathology of the disease is not completely understood. Identification of somatic mutations in *JAK2*, *CALR*, or *MPL* in nearly 90% of patients with PMF underscores the central role of the JAK/STAT pathway activation in the disease.[2] Although JAK inhibitors provide symptomatic relief and a limited survival benefit,[3-6] allogeneic stem cell transplantation remains the only curative treatment option. However, only the

youngest patients are eligible, given the high toxicity of this approach.[7] Novel therapeutic strategies are thus needed.

Several cytokines are suspected to be abnormally produced and contribute to PMF pathogenesis. Among these, TGF-β1 has received much attention owing to its profibrotic properties that contribute to PMF in several murine models.[8-11] However, the cell types that produce the pathogenic TGF-β1 in PMF is unknown.

Virtually all cell types produce TGF-β1 in a latent, inactive form. In latent TGF-β1, the mature TGF-β1 dimer remains noncovalently associated with the latency associated peptide (LAP), which forms a ring around the mature TGF-β1 and masks sites of interaction with the TGF-β receptor. To exert activity, mature TGF-β1 must be released from LAP, a process referred to as TGF-β1 activation. Only a few cell types were shown to activate TGF-β1 via molecular mechanisms that are cell type-specific. In stimulated regulatory T lymphocytes (Tregs), the transmembrane protein GARP binds to LAP by disulfide linkage,

allowing the presentation and activation of latent TGF-β1 on the Treg surface by integrin αVβ8.[12-17] GARP:(latent)TGF-β1 complexes are also expressed on the surface of B cells, MKs, and platelets.[18,19] Upon stimulation, B cells and platelets release active TGF-β1 from surface GARP:TGF-β1 complexes, but the other protein that contributes to TGF-β1 activation by these cells is not fully elucidated.[20]

We previously derived anti-human or mouse GARP:TGF-β1 monoclonal antibodies (mAbs) that block TGF-β1 activation by GARP-expressing cells in vitro and in vivo.[15,17] The anti-GARP:TGF-β1 clone 58A2 blocked TGF-β1 activation and immunosuppression by mouse Tregs and induced an immune-mediated rejection of mouse tumors when combined with anti–PD-1.[17] The antibody-mediated GARP:TGF-β1 blockade is currently being tested in patients with locally advanced or metastatic solid tumors (ClinicalTrials.gov: NCT03821935).

Here, we hypothesized that pathogenic TGF-β1 is produced by GARP-expressing cells during PMF development and we tested whether anti-GARP:TGF-β1 could exert therapeutic activity in a murine model of the disease.

Methods

Retroviruses

HEK293-EBNA cells were transfected with pMegix-MPL^{W508A}–internal ribosome entry site– green fluorescent protein (IRES-GFP) or pMegix-MPL$^{Wild Type (WT)}$-IRES-GFP and packaging plasmids. Supernatants were collected within 72 hours and concentrated from 60 to 100× on Centricon Plus 70 columns (Merck Millipore, UFC703008). Titers of retroviral stocks were determined by fluorescence-activated cell sorting analysis of GFP expression 48 hours after spin infection (300g for 2 hours at 37°C) of 293T cells in the presence of Polybrene (8 μg/mL).

Mouse experiments

C57BL/6J, Vav^{Cre} × JAK2$^{L2/WT}$, Tg(Pf4^{Cre}) × Garp$^{fl/fl}$, and Foxp3^{Cre} × Garp$^{fl/fl}$ mice were bred at the specific pathogen free animal facility of UCLouvain. Tg(Pf4^{Cre}) × Garp$^{fl/fl}$ and Foxp3^{Cre} × Garp$^{fl/fl}$ mice were kindly provided by Wim Maes (KULeuven). UBC-GFP mice (C57BL/6-Tg(UBC-GFP)$^{30Scha/J}$) were purchased from Jackson Laboratory. Animal studies were performed in accordance with national and institutional guidelines, under permit numbers 2017/UCL/MD/019 and 2019/UCL/MD/032. MPL^{W508A} and MPL^{WT} mice were generated by BM transplantation. Donor mice were injected with 5-fluorouracil [5-FU, 3 mg intraperitoneal (IP)] to increase the proportion of cycling HSCs. After 4 days, BM cells were flushed from femurs and tibias and passed through 70 μm nylon meshes. After red blood cell lysis, BM cells were stimulated with murine fms-like tyrosine kinase 3-ligand, stem cell factor, interleukin-3, interleukin-6, and thrombopoeitin (10 ng/mL each, all from Miltenyi) for 24 hours in α-MEM (Gibco # 32561-029). Spin infections (300g for 2 hours at 37°C) were performed at a 5:1 retrovirus-to-cell ratio in the presence of Polybrene (8 μg/mL). Cells were incubated for an additional 48 hours in the presence of retrovirus and cytokines, then collected, washed, and injected retro-orbital into lethally irradiated (2 × 500 centigray) recipients (2 × 10^5 cells per mouse). In some experiments, BM cells were isolated from donors that had not received 5-FU and transplanted without prior retroviral transduction into lethally irradiated recipients (2 × 10^6 cells per mouse). In competitive transplantation experiments, BM cells were isolated from Vav^{Cre} × JAK2$^{L2/WT}$ and UBC-GFP donors (no 5-FU), mixed at a 1:1 ratio, and transplanted into lethally irradiated UBC-GFP recipients (3 × 10^6 BM cells per mouse). Where indicated, recipients received weekly injections (400 μg per mouse IP) of an isotype control (motavizumab, mIgG2a) or anti-GARP:TGF-β1 (clone 58A2, mIgG2a, WT, or Fc-Dead), starting 1 day before transplantation. To deplete CD8$^+$ T cells, recipients received anti-mouse CD8α (Bio X Cell, clone 2.43) on days −2 and 0 of transplantation (500 μg per mouse IP), then weekly (250 μg per mouse IP) thereafter. Blood samples were collected weekly for cell counting and flow cytometry. Mice were euthanized, at the end of the experiment (days 32-34, as indicated), to collect spleen and femurs for histopathology, western blot, flow cytometry, and RNA sequencing (RNAseq [see supplemental Material for detailed methods, available on the Blood website]).

Human PBMC samples

Whole blood samples from patients initially diagnosed with PMF or from patients with post–essential thrombocythemia/polycythemia vera PMF who were treated following the clinical practice guidelines were collected at the follow-up consultations. All patients provided written informed consent. The study was approved by the Commission d'Ethique Biomédicale Hospitalo-Facultaire, Brussels, Belgium (reference CEHF 2019/21NOV/518). Peripheral blood mononuclear cell (PBMC) isolation and analyses by flow cytometry are described in supplemental Methods.

RNAseq analyses

In Figure 5, 58A2-treated mice were considered as responders if their MPL^{W508A}/GFP$^+$ white blood cell (WBC) count was inferior compared with the median WBC count (<3.8 × 10^4/μl). Nonresponders had MPL^{W508A}/GFP$^+$ WBC counts similar to that of the isotype control group and were excluded to avoid biased effect sizes and to identify transcriptional changes associated with a measurable therapeutic effect. Spleens were disrupted using Ultra Turrax (Ika). Total RNA was extracted using the NucleoSpin RNA kit (Macherey Nagel, 740955.50). RNA quality was verified using Agilent Bioanalyzer, and sequencing was performed via Macrogen using Illumina SBS technology (paired-end reads; 30 million reads/sample). Sequences were aligned to the GRCm38 mouse genome using the STAR software (www.star.mit.edu), and read counts were determined with the HTSeqCount software. Raw read counts were normalized using the DESeq2 package[21] and the R software. Gene set enrichment analyses (GSEAs) were performed on normalized read counts using the GSEA Software.[22] Molecular Signature Database v7.2 (MSigDB) was used for hallmark signatures[23], and Panglao Database for cell-type signatures.[24] Of the 178 existing cell-type signatures in Panglao, 60 were excluded because of small gene set size (<15). The mouse fibrosis signature was extracted from published results.[25]

Statistical analyses

Statistical analyses were performed using GraphPad Prism software (version 9). Differences between groups were compared using unpaired two-tailed t test (for blood cell

counts), or unpaired two-tailed Mann–Whitney test (for fibrosis scores and TGF-β1 concentrations in the serum). The threshold for statistical significance was 0.05.

Results

Increased GARP levels in the BM and spleen of mice with PMF

TGF-β1 is thought to be pathogenic and contribute to fibrosis in PMF, but the cells that produce and activate the cytokine during disease progression is unknown. GARP-expressing cells are interesting candidates because the TGF-β1 activation by these cells, but not by other cells, can be blocked with anti-GARP:TGF-β1 mAbs. We thus examined whether GARP-expressing cells are present or enriched in the BM and spleen of mice with PMF.

Most clinical features observed in patients with PMF, including leukocytosis, splenomegaly, and BM and spleen fibrosis, can be induced in mice by transplanting syngeneic BM cells retrovirally transduced to express a constitutively active mutant TPO receptor (MPL^W508A), the homolog of the pathogenic human MPL^W515A variant. Expression of MPL^W508A in BM cells activates the JAK/STAT pathway.[26,27] Here, briefly, BM cells were isolated from 5-FU treated C57BL/6 mice, transduced with a retroviral vector encoding MPL^W508A and GFP (Mpl^W508A-IRES-GFP), and transplanted into lethally irradiated C57BL/6 recipients (Figure 1A). Transduction efficacy ranged from 5% to 15% according to the GFP expression. Severe leukocytosis developed within 14 to 28 days after transplantation of BM cells transduced with Mpl^W508A-IRES-GFP, but not with Mpl^WT-IRES-GFP, taken as controls here (supplemental Figure 1A). We will refer to these mice as MPL^W508A or MPL^WT controls, respectively. Leukocytosis reflects the proliferation of transformed MPL^W508A/GFP^+ cells. It is accompanied by the development of spleen and BM fibrosis measured by the histological analyses of organs collected 4 to 5 weeks after transplantation (supplemental Figure 1B). Phosphorylated STAT5 (pSTAT5) levels were higher in BM and splenocytes of MPL^W508A mice than in BM and splenocytes of MPL^WT controls, confirming the constitutive activation of the JAK/STAT pathway in this murine model of PMF (Figure 1B).

GARP protein levels were significantly higher in BM and spleen of MPL^W508A mice than in those of the controls (Figure 1B). Tregs (FOXP3^+ cells) and MKs (CD41^high cells) represented the vast majority (>95%) of GARP-expressing cells in these organs (supplemental Figure 2A) and virtually all Tregs and MKs expressed GARP (supplemental Figure 2B). Nearly all GARP^+ cells were Tregs in the BM and spleen of MPL^WT mice, whereas Tregs represented only ~50% of GARP^+ cells in MPL^W508A mice, with MKs representing the other ~50% (supplemental Figure 2A). Altogether, the proportions of GARP^+ Tregs within live cells reduced 2- to 3-fold, but proportions of GARP^+ MKs increased 20- to 30-fold in MPL^W508A mice in comparison with that in the controls (Figure 1C). Increased proportions of MKs in BM and spleen were expected because the activation of the JAK/STAT pathway in PMF drives differentiation and proliferation of myeloid cells, notably MKs. Increased proportions of MKs, combined with very high expression of GARP per single MK (supplemental Figure 2B) most likely accounts for the

observed increase in GARP protein levels in the BM and spleens of MPL^W508A mice (Figure 1B). As expected, all MKs were GFP^+, indicating that they originated from transformed cells expressing MPL^W508A, whereas Tregs were GFP^-, indicating that they mostly originate from non-transformed lymphoid progenitors (Figure 1D).

Altogether, the results above show that in mice undergoing MPL^W508A-induced PMF, GARP-expressing cells are present and GARP levels are increased in the BM and spleen as a consequence of increased proportions of tumoral GARP^+ MKs.

A blocking anti-GARP:TGF-β1 mAb reduces tumor burden in mice with PMF

Next, we explored whether blocking TGF-β1 activation by GARP-expressing cells could exert a therapeutic activity in PMF. We used the anti-GARP:TGF-β1 clone 58A2 (mouse immunoglobulin G2a [mIgG2a]), which was shown to block TGF-β1 activation by mouse Tregs.[17] We first verified that 58A2 also blocks TGF-β1 activation by mouse platelets, which are easier to isolate than MKs. Production of active TGF-β1 in mouse serum during blood coagulation in vitro was significantly reduced in the presence of 58A2 (supplemental Figure 3). Next, we administered 58A2 weekly to the MPL^W508A and MPL^WT mice, starting 1 day before the BM transplantation. On comparison with the mIgG2a isotype control, 58A2 reduced spleen and BM fibrosis measured on day 34 in MPL^W508A mice, although this did not reach statistical significance (Figure 2A). Unexpectedly, 58A2 significantly reduced the tumor burden in MPL^W508A mice: counts of total (GFP^+ and ^-) platelets and WBCs were markedly reduced (Figure 2B). This reduction was due to reduced numbers of tumoral MPL^W508A/GFP^+ cells and, notably, GFP^+ neutrophils, which accounted for the majority of the GFP^+ WBCs in MPL^W508A mice. Counts of nontransduced GFP^- WBCs, neutrophils, and platelets were not reduced. The GARP:TGF-β1 blockade by 58A2 did not reduce counts of nontumoral MPL^WT/GFP^+ or ^- cells in MPL^WT controls, which did not develop pathological leukocytosis or fibrosis (Figure 2A-B). In line with this, no reduction in WBC and platelet counts was observed in mice transplanted with nontransduced BM cells and treated with 58A2, in comparison with the isotype control (supplemental Figure 4).

Altogether, our results suggest that anti-GARP:TGF-β1 reduces tumor burden in murine PMF by selectively killing or limiting the expansion of MPL^W508A-transformed cells.

Reduced tumor burden in PMF does not require the effector functions of anti-GARP:TGF-β1

58A2 could reduce tumor burden in PMF by killing tumoral GARP^+ cells via antibody-dependent cellular cytotoxicity or phagocytosis. To test this possibility, we used an Fc-dead version of 58A2 containing D265A/N297A substitutions in the Fc region that preclude binding to mouse FcγRs. We previously showed that Fc-dead 58A2 exerts antitumor activity against CT26 and MC38 tumors as efficiently as wild-type 58A2.[17] As shown in Figure 3A, the tumor burden and fibrosis in MPL^W508A mice were reduced to similar levels upon treatment with wild type or Fc-dead 58A2, indicating that the therapeutic effects of anti-GARP:TGF-β1 in PMF did not require antibody binding to
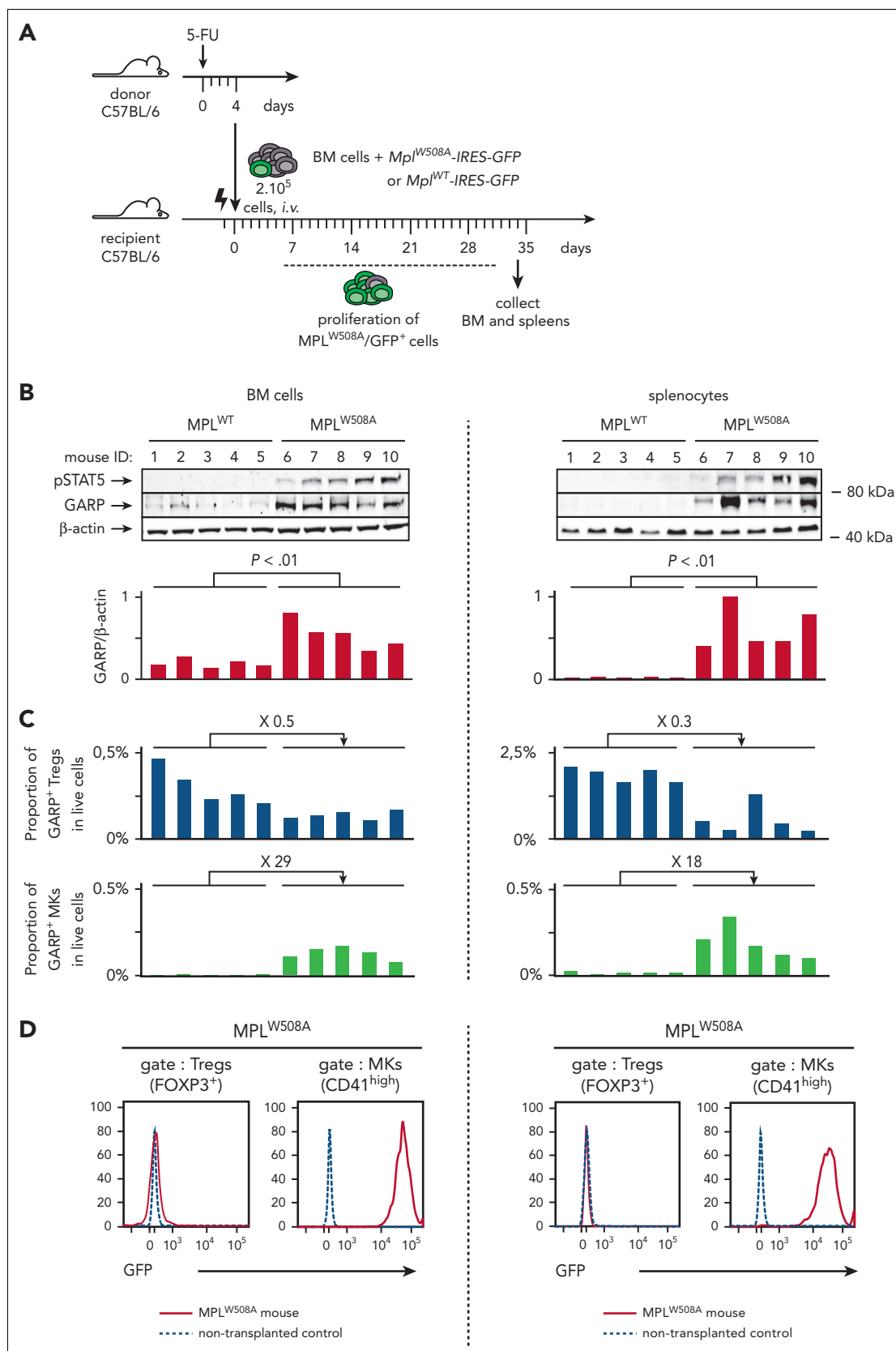
Figure 1. GARP protein is increased in murine PMF and is expressed exclusively on MKs and Tregs. (A) Schematic representation of the experimental design. BM cells were isolated from 5-FU-treated donor mice, transduced with a retrovirus encoding MPL[W508A] or MPL[WT] and transplanted into lethally irradiated recipient mice (n = 5 mice/group). BM cells and splenocytes were isolated from MPL[W508A] or MPL[WT] control mice 34 days after transplantation. (B) Western blot analyses of BM cells and splenocytes with antibodies against GARP, pSTAT5, or β-actin. Bar graphs show quantification of enhanced chemiluminescence signals. P values were calculated using a two-tailed

FcγRs and thus, did not imply killing of GARP⁺ tumor cells by antibody-dependent cellular cytotoxicity or phagocytosis.

Reduced tumor burden may result from reduced cytostasis exerted by TGF-β1 on normal hematopoietic progenitors

Alternatively, 58A2 could reduce the cytostasis exerted by TGF-β1 on nontransformed hematopoietic progenitors, favoring their proliferation and, in turn, reducing the competitive growth advantage of malignant cells that are resistant to TGF-β1 cytostasis. Resistance to TGF-β1 cytostasis was suggested to favor transformed cell expansion in mouse and human PMF.[29-31] We observed that the expression of constitutively active MPL^W508A, but not MPL^WT, reduced the ability of recombinant TGF-β1 to suppress the proliferation of murine myeloid 32D cells in vitro (Figure 3B). This was true using transduced 32D cells or clones, in the absence or presence of IL-3 or TPO, and similar observations were made with murine myeloid Ba/F3 cells transduced to express the constitutively active human MPL^W515K mutant (Figure 3B; supplemental Figure 5). Thus, our results show that the constitutive activation of the JAK/STAT pathway by mutant MPL in myeloid cells induces resistance to the cytostatic effects of TGF-β1 in vitro. It remains to be determined whether this mechanism contributes to the therapeutic effect of GARP:TGF-β1 blockade in murine or human PMF.

Targeting GARP:TGF-β1 complexes on Tregs reduces tumor burden in murine PMF

Tregs and MKs represent the vast majority of GARP-expressing cells in the spleen and BM of mice undergoing PMF. To define which GARP-expressing cells need to be targeted by anti-GARP:TGF-β1 to observe therapeutic effects, we induced PMF in mice carrying a Treg- or an MK/platelet–specific deletion of the Garp gene.[17]

In preliminary experiments with UBI-GFP BM donor cells, 100% of MKs and platelets (CD41⁺) were of donor origin as early as 19 days after transplantation. However, more than 50% of Tregs (CD4⁺GARP⁺) were still of recipient origin on day 36, when full reconstitution was achieved (supplemental Figure 6A-C). This is due to the known resistance of T cells to irradiation, in comparison to that of B cells and myeloid cells ([32] and supplemental Figure 6D). Thus, to ensure that all Tregs (donor and recipient origin) carry a deletion of Garp in MPL^W508A mice, BM cells from Foxp3^Cre × Garp^fl/fl mice were transduced with Mpl^W508A-IRES-GFP and transplanted into irradiated Foxp3^Cre × Garp^fl/fl recipients. PMF in these mice was compared with that induced by transplanting transduced BM cells from Foxp3^Cre × Garp^wt/wt donors into Foxp3^Cre × Garp^wt/wt recipients. Similar to what was observed by blocking GARP:TGF-β1 with a mAb, counts of transformed MPL^W508A/GFP⁺ WBC were significantly reduced in the absence of GARP:TGF-β1 on Tregs (Figure 4A). MPL^W508A/GFP⁺ platelet counts and fibrosis were also reduced, although this did not reach statistical significance.

Next, we transplanted transduced BM cells from MK/platelet–specific Garp knockout (KO) [Tg(Pf4^Cre) × Garp^fl/fl] or WT littermates (Garp^fl/fl) into WT recipients (Garp^fl/fl). WT recipients could be used in the 2 conditions because all MKs and platelets are from donor origin early after transplantation. In contrast to the observations with Treg-specific Garp KOs, tumor burden was not reduced in MPL^W508A mice transplanted with MK/platelet–specific Garp KO cells, when compared with that in WT mice (Figure 4B).

Altogether, our results suggest that anti-GARP:TGF-β1 mAb reduces tumor burden in PMF by blocking GARP:TGF-β1 on Tregs, but not on MKs or platelets. This was unexpected. While a role for MKs in PMF pathogenesis is well established,[33,34] a role for Tregs has not been reported. A plausible hypothesis to explain our observations is that Tregs suppress antitumor T-cell responses in PMF, as they do in many types of human or murine cancers, and this immunosuppression is relieved at least in part by GARP:TGF-β1 blockade.

GARP:TGF-β1 blockade during PMF increases interferon-γ (IFNγ) signals in spleen

We used RNAseq to confirm the effects of 58A2 on tumor burden and fibrosis, and tested the hypothesis that GARP:TGF-β1 blockade could relieve suppression of T cell-mediated antitumor immunity by Tregs.

RNAseq of spleens collected from nontreated MPL^W508A mice on days 13 and 20 were compared to establish signatures of PMF progression. The RNAseq of spleens collected on day 34 from MPL^W508A mice responding to 58A2 were compared with that of nontreated controls to analyze effects of treatment with 58A2 (Figure 5A). We performed GSEA[22] of genes ordered according to the fold-change expression during PMF progression (day 20 vs 13 in controls), or according to the fold-change expression in response to treatment (58A2 responders vs controls on day 34).

As shown in Figure 5B (white bars), 5 myeloid cell-specific gene signatures from the PanglaoDB[24] and a signature of murine MF[25] showed a significant positive enrichment during PMF progression [enrichment score (ES) > 0.4 and false discovery rate (FDR) <5%]. The same signatures were negatively enriched in 58A2 responders (ES < −0.4 and FDR < 5%; black bars in Figure 5B). Thus, GSEA detects progression of tumor burden and fibrosis between days 13 and 20 in nontreated controls and reduced tumor burden and fibrosis on day 34 in responders vs in controls.

We then used the 50 hallmark signatures from the MSigDB database[23] to search for the mechanisms of actions by which 58A2 could exert this antitumor activity. Five and 6 hallmark signatures were positively or negatively enriched in 58A2 responders, respectively. Reverse enrichments were observed during PMF progression in controls (Figure 5B). Signatures that were negatively enriched in responders comprised hallmarks of

---

Figure 1 (continued) Student t test. (C) Proportions of GARP⁺ Tregs and GARP⁺ MKs in live single cells, as determined by flow cytometry. Fold differences between mean proportions in MPL^W508A and MPL^WT mice are indicated above bar graphs. (D) Histograms showing GFP expression on Tregs and MKs in the BM and spleen from 1 representative MPL^W508A mouse. Cells from a C57BL/6 mouse that did not undergo transplantation were used as negative controls. The experiment is representative of at least 3 other independent experiments.
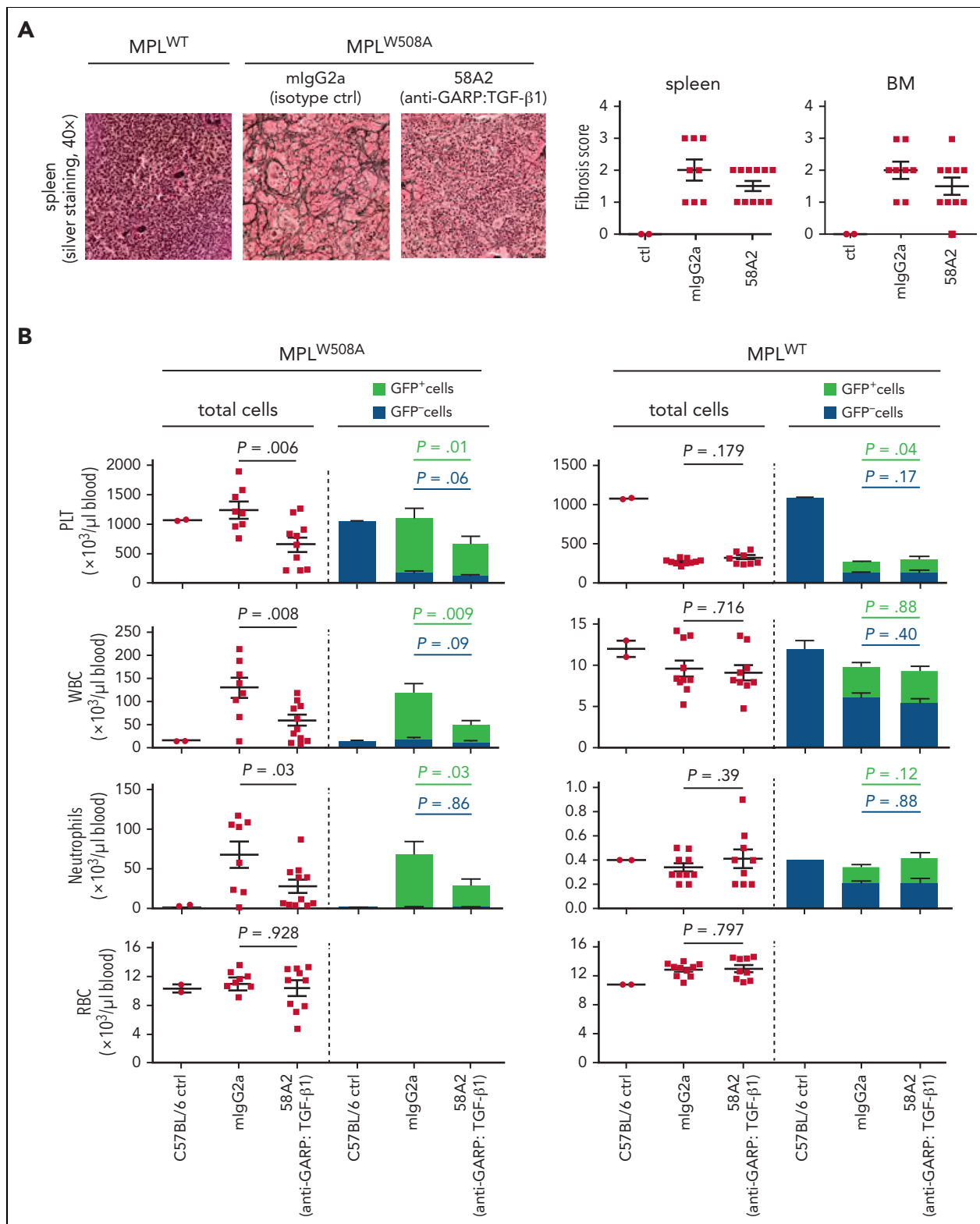
Figure 2. Blocking anti-GARP:TGF-β1 mAbs reduces fibrosis and tumor burden in murine PMF. MPL^W508A and MPL^WT control mice, generated as indicated in Figure 1, were injected IP weekly with the indicated mAbs, starting 1 day before transplantation of the transduced BM cells (n = 8-10 mice per group). C57BL/6 mice that did not undergo transplantation served as additional controls (ctrl). Blood was taken on day 28 and mice were euthanized on day 34 to collect femurs and spleens. (A) Histological assessment of fibrosis in sections of paraffin-embedded spleens and femurs after silver staining. Representative sections are shown on the left. Fibrosis scores, corresponding to reticulin staining grades expressed on a modified Bauermeister scale,[28] are indicated on the right. Data points: scores in individual mice; horizontal bars: mean + SEM per group. (B) Blood cell counts and GFP expression were determined using a hematological analyzer and flow cytometry. Data points on the left: blood cell counts in individual mice; horizontal bars: mean + SEM per group. Stacked bar graphs on the right: mean + SEM of GFP+ and GFP- cells. Data from 1 of at least 4 independent experiments. P values calculated using a two-tailed Student t test. SEM, standard error of the mean.
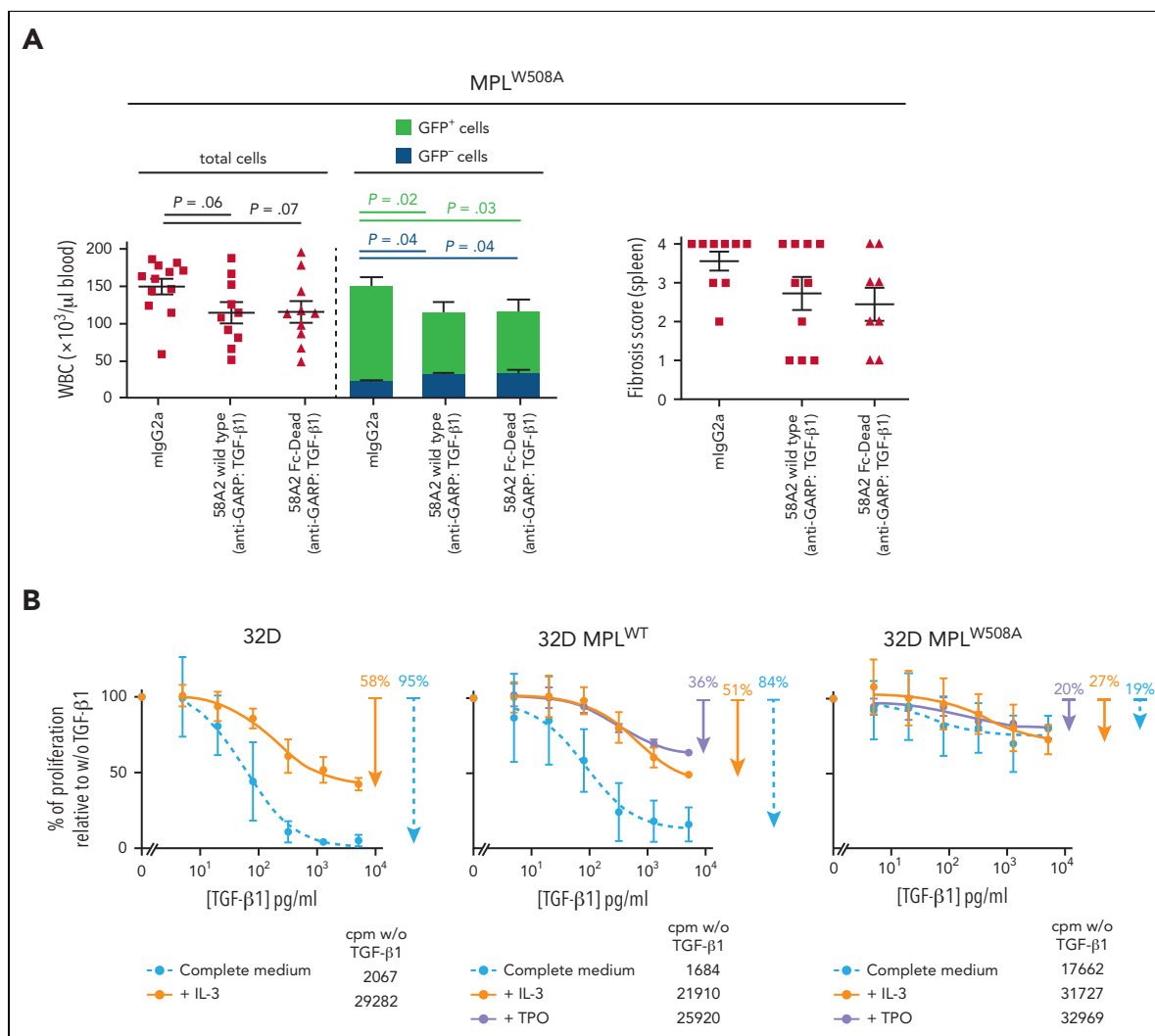
Figure 3. Reduced tumor burden and fibrosis in PMF do not require effector functions of anti-GARP:TGF-β1 mAbs. (A) MPL^W508A mice were treated with wild-type or Fc-dead mAbs as indicated in Figure 2 (n = 8-10 mice per group). Blood was taken on day 21 and mice were euthanized on day 32 to collect femurs and spleens. Blood cell counts, GFP expression, and spleen fibrosis were measured as indicated in Figure 2. Data points: values in individual mice; horizontal lines: mean ± SEM per group; stacked bars: mean + SEM. P values were calculated using a two-tailed Student t test. (B) 32D cells were transduced with *Mpl^WT-IRES-GFP* or *Mpl^W508A-IRES-GFP* RV and GFP+ cells were sorted by flow cytometry. Parental 32D cells, sorted MPL^WT/GFP+, or MPL^W508A/GFP+ bulk cell populations, or clones (supplemental Figure 6) were cultured in complete medium, in the absence or presence of recombinant IL-3, TPO, or TGF-β1, as indicated in the graphical legend. Proliferation was measured in ³H-thymidine incorporation assays. Maximum growth inhibition (%) in the presence of rTGF-β1 is indicated in colored text on the right and was calculated as follows: (cpm w/o rTGF-β1 − cpm at the highest concentration of rTGF-β1) ÷ (cpm w/o rTGF-β1). Data points: mean cpm ± SD (triplicates). Results are representative of 2 independent experiments. cpm w/o rTGF-β1, counts per minute in the absence of rTGF-β1; SD, standard deviation.

platelet components or functions (coagulation), fibrotic processes (epithelial to mesenchymal transition), and inflammation (inflammatory response and IL6 JAK STAT3 signaling), again likely reflecting reductions in tumor burden, fibrosis or other PMF features, such as inflammation in response to treatment.[34,35] Less expected were the hallmarks of IFNα and IFNγ signaling, which were positively enriched in responders (Figure 5B). Genes composing the IFNα and IFNγ signatures partially overlap, but 43% of the genes in the leading edge of the IFNγ signature are not present in the IFNα signature (Figure 5C). Levels of IFNγ- and/or IFNα-induced mRNAs inversely correlated with MPL^W508A/GFP+ WBC counts, suggesting an association between increased interferon signaling and decreased tumor burden (Figure 5D).

Finally, negative enrichments for signatures of TGF-β1 signaling in CD4+ T cells and fibroblasts[13,36] were also found in responders, even though they did not reach statistical significance (FDR = 7.6% and 10.6%) (Figure 5B).

Altogether, the analyses of transcriptional profiles in murine PMF confirmed reduced disease burden in response to the GARP:TGF-β1 blockade, but it also suggested that therapeutic activity of 58A2 is associated with reduced TGF-β1− and increased interferon− signals. Reduced TGF-β1 activity was expected as 58A2 blocks TGF-β1 activation by GARP-expressing cells, such as Tregs. Increased interferon signals may indicate increased T-cell activity resulting from reduced Treg immunosuppression.
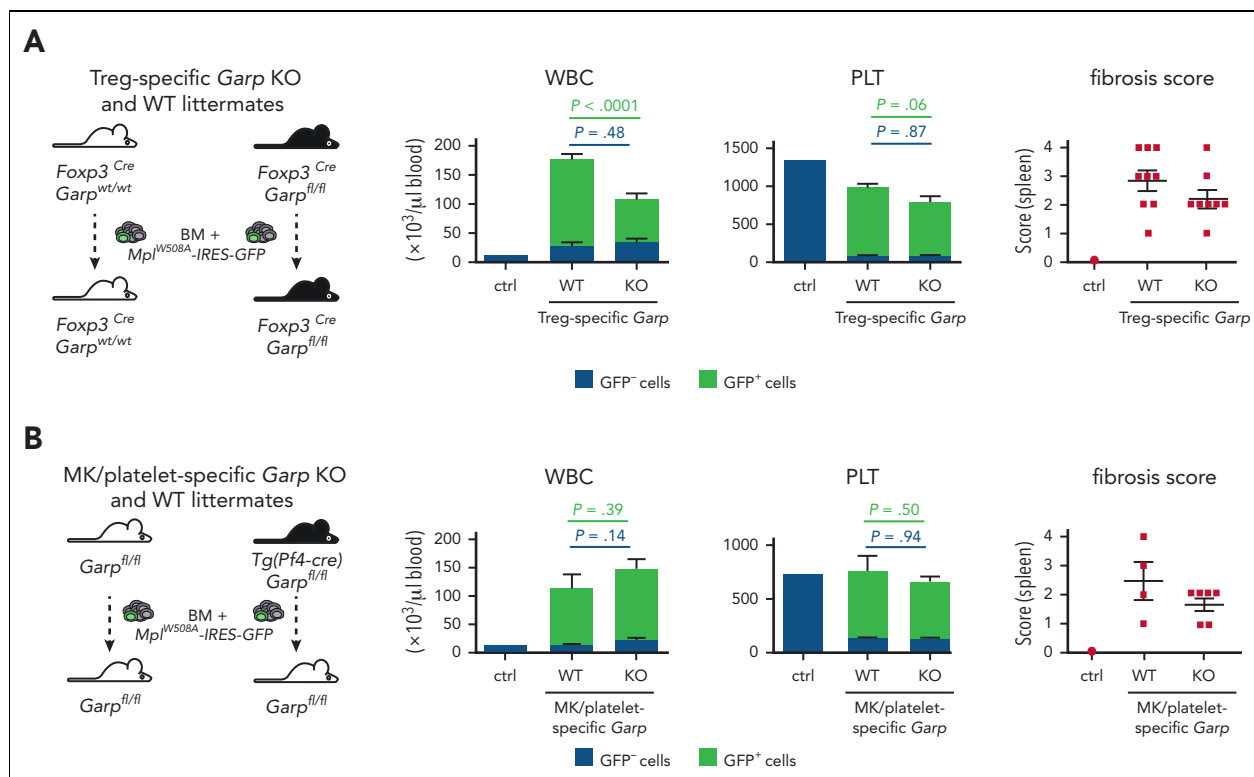
Figure 4. Absence of GARP:TGF-β1 complexes on Tregs, but not on MKs, reduces fibrosis and tumor burden in PMF mouse models. (A) BM cells were isolated from 5-FU-treated $Foxp3^{Cre} \times Garp^{wt/wt}$ mice or $Foxp3^{Cre} \times Garp^{fl/fl}$ mice, transduced with a retrovirus encoding MPL^{W508A}, and transplanted into irradiated recipient mice of the same genotype as the donor mice (n = 8-9 mice per group). C57BL/6 mice that did not undergo transplantation were used as controls. Blood was taken on day 28 and mice were euthanized on day 34 to collect femurs and spleens. Blood cell counts, GFP expression, and spleen fibrosis were measured as indicated in Figure 2. Data points: values in individual mice; horizontal lines: mean ± SEM per group; stacked bars: mean + SEM. P values were calculated using a two-tailed Student t test. (B) Same as in (A), except that BM cells were isolated from $Garp^{fl/fl}$ or $Tg(Pf4^{Cre}) \times Garp^{fl/fl}$ mice and transplanted into irradiated $Garp^{fl/fl}$ recipients (n = 4-6 mice per group).

Therapeutic efficacy of anti-GARP:TGF-β1 mAbs in PMF requires CD8⁺ T-cell function

We previously observed in CT26-bearing mice that blocking GARP:TGF-β1 on Tregs increased IFNγ production by antitumor CD8⁺ T cells.[17] To test the involvement of CD8⁺ T cells in the therapeutic activity of the GARP:TGF-β1 blockade in PMF, we depleted these cells by repeated injections of an anti-CD8α mAb (Figure 6A; supplemental Figure 7). CD8⁺ T-cell depletion abolished the reduction of MPL^{W508A}/GFP⁺ neutrophil counts obtained with 58A2 (Figure 6B). It had no effect in mice that did not receive 58A2, which was expected because PMF develops very rapidly in this model, leaving little opportunity for spontaneous antitumor CD8 T cells to control the disease. Thus, the therapeutic efficacy of 58A2 in murine PMF requires CD8⁺ T cells.

## GARP:TGF-β1 blockade reduces tumor burden in another murine model of MPN

We tested whether 58A2 could exert antitumor activity in a non-PMF model of MPN. BM cells from mice carrying a heterozygous $JAK2^{V617F}$ knockin mutation in HSCs[37] were mixed at a 1:1 ratio with BM cells from UBI–GFP mice and transferred into irradiated UBI–GFP recipients (supplemental Figure 8A). Recipients developed a moderate form of MPN that resembles polycythemia vera more than PMF and includes mild erythrocytosis, thrombocytosis, and leukocytosis. 58A2 significantly reduced WBC counts in recipient mice, but not red blood cells

and platelets (supplemental Figure 8B). Reduction in WBCs was mostly in $JAK2^{V617F/WT}$ (GFP⁻) neutrophils (supplemental Figure 8C). Counts of other $JAK2^{V617F/WT}$ myeloid cells, including monocytes, eosinophils, and basophils, were also reduced, although this did not reach statistical significance. Counts of $JAK2^{WT/WT}$ myeloid cells and $JAK2^{V617F/WT}$ or $JAK2^{WT/WT}$ lymphocytes were not modified (supplemental Figure 8C). These results suggest that GARP:TGF-β1 blockade may also reduce tumor burden in non-PMF MPNs.

GARP is expressed on the surface of stimulated Tregs and platelets isolated from the blood of patients with MF

We isolated human PBMCs from the blood of patients with MF or from hemochromatosis, non-MF controls. Cells were stained immediately or after a short stimulation of T cells in vitro to analyze surface GARP expression using flow cytometry. As expected, GARP was not detected on unstimulated T cells (CD8⁺, CD4⁺, or Tregs), but its expression was induced by the T-cell receptor stimulation on CD4⁺FOXP3⁺ T cells (ie, mostly Tregs). GARP-expressing Tregs comprised 30.4 ± 12.5% (mean ± SD) of all CD4⁺FOXP3⁺ cells in patients with MF and control patients, with no significant difference between the 2 groups. We also examined GARP expression on platelets that were co-purified with PBMCs (FSC^{low}CD41⁺ events): a vast majority expressed GARP, with no difference between control patients with or without MF (supplemental Figure 9). We
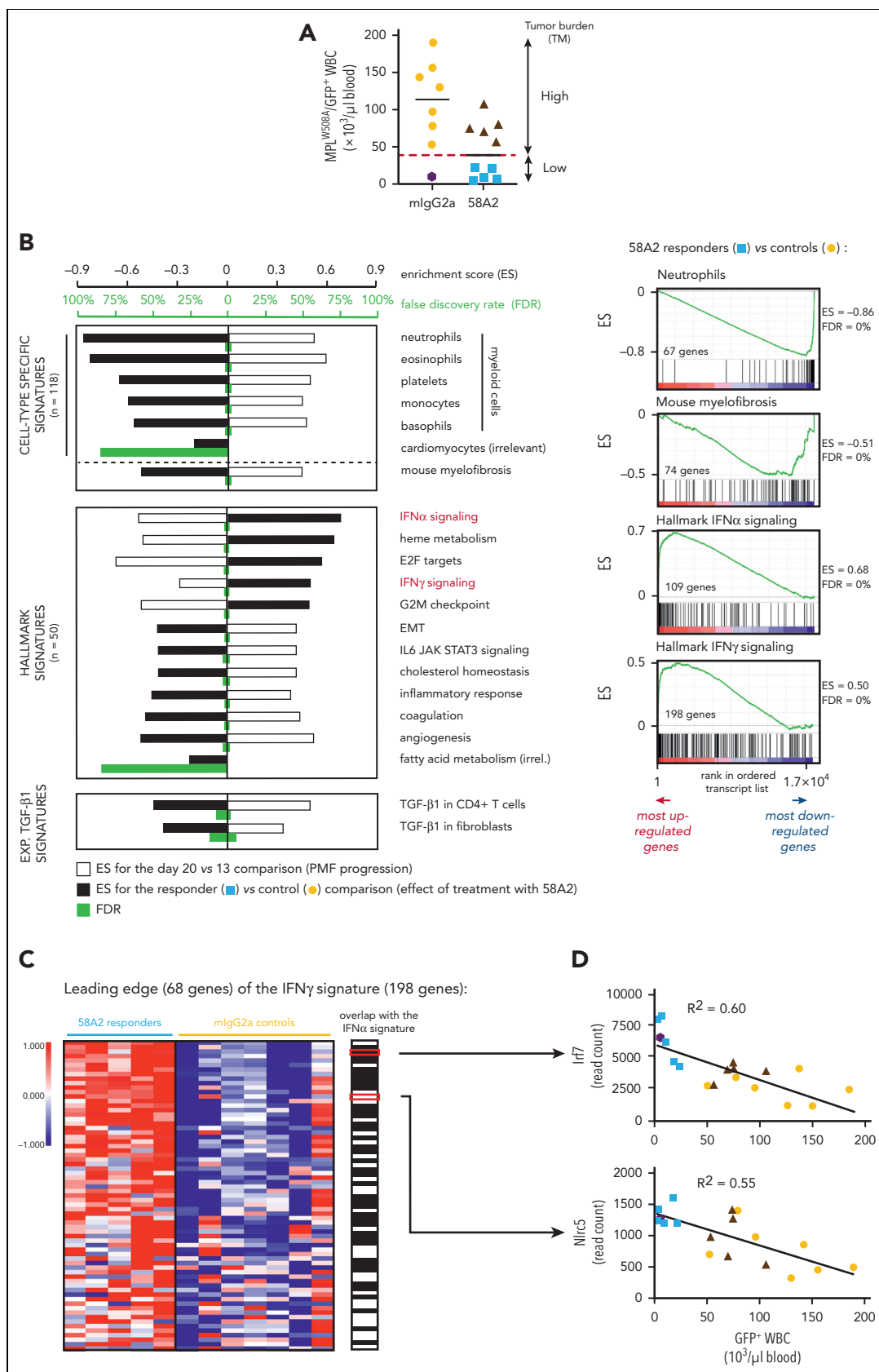
Figure 5. Anti-GARP:TGF-β1 mAbs induce an IFNγ signature in murine PMF. (A) MPL[W508A]/GFP[+] WBC counts on day 34 in mice from experiment in Figure 2. Data points: individual mice; horizontal lines: median + SEM per group. MPL[W508A] mice responding to 58A2 (n = 5, blue symbols) are defined as mice with a low tumor burden (cut-off: median MPL[W508A]/GFP[+] WBC counts in the 58A2 group). Controls correspond to nontreated (mIgG2a) MPL[W508A] mice with a high tumor burden (n = 7, orange symbols). (B) GSEA of RNAseq data from spleens collected from MPL[W508A] mice on days 13, 20, or 34. White bars: ES of the indicated signatures in the list of transcripts ordered by mean
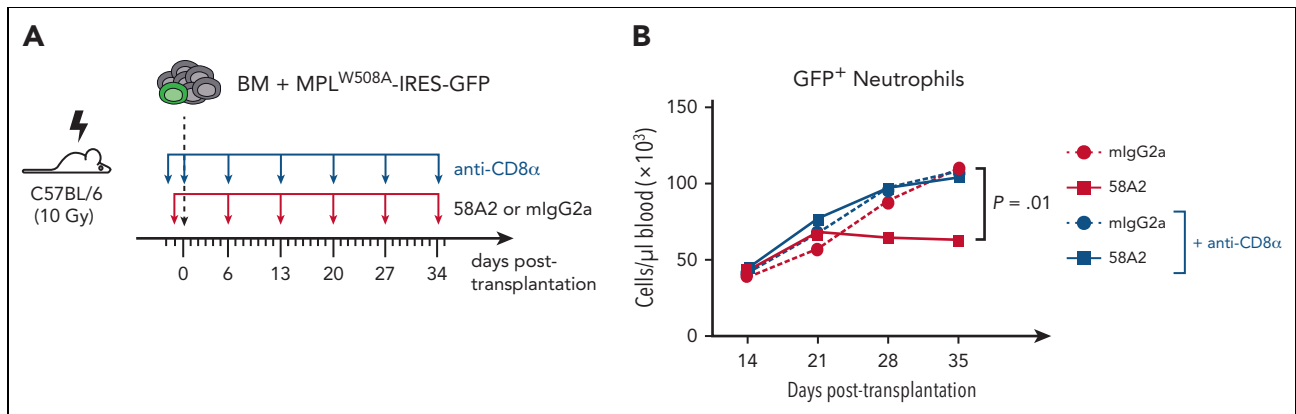
Figure 6. Therapeutic efficacy of anti-GARP:TGF-β1 mAb in murine PMF requires T cell function. (A) Recipient mice were transplanted with transformed MPL^W508A/GFP+ cells and injected IP weekly with 58A2 and/or anti-CD8α mAbs at the time points indicated. Blood samples were collected weekly starting on day 14 for blood cell count and flow cytometry. Mice were euthanized on day 35. (B) Counts of GFP+ blood neutrophiles during PMF progression. Data points: mean values per group (n = 6-8 mice per group). P values were calculated with a repeated measure analysis of variance.

concluded that cellular targets of anti-GARP:TGF-β1 mAbs are found in the blood of patients with MF. Altogether, our results suggest that GARP:TGF-β1 blockade warrants testing as a novel therapeutic strategy for MPNs, most particularly MF.

Discussion

The effects of GARP:TGF-β1 blockade on tumor burden in murine PMF are the most important results of this report. They were completely unexpected, as our hypothesis was that the GARP:TGF-β1 blockade would reduce fibrosis owing to the previously reported profibrotic roles of TGF-β1 in PMF.[8-11] We repeatedly observed reductions in spleen and BM fibrosis, but it did not reach statistical significance and may be secondary to the significant tumor burden reduction in response to treatment. Thus, although we do not exclude a direct profibrotic role for TGF-β1 in PMF, our data suggest that TGF-β1 exerts deleterious effects by favoring the clonal expansion of transformed cells. In homeostatic conditions, TGF-β1 reduces hematopoiesis. It imposes cytostasis on normal BM progenitors, maintaining them in a state of quiescence to prevent exhaustion.[38-41] Recent studies suggested that in MPNs, malignant cells fail to respond to the cytostatic activity of TGF-β1, which could even promote their proliferation, either directly or competitively by decreasing the growth of normal HSCs.[30,31] In these studies, the clonal dominance of JAK2^V616F cells over WT cells in competitive transplantation assays was abrogated by the genetic deletion of the TGF-βRII receptor in WT cells but not in JAK2^V616F cells.[31] Here, we observed that expression of mutant MPL^W508A in murine myeloid cells induced resistance to the cytostatic effect of TGF-β1. Thus, the antitumor activity of the GARP:TGF-β1 blockade in PMF could result from the reactivation of normal hematopoiesis and competition with transformed cells. A direct antiproliferative effect of the GARP:TGF-β1 blockade on transformed cells, via a mechanism not yet determined, cannot be excluded.

A second unexpected result is that tumor burden reduction in response to the GARP:TGF-β1 blockade depends on GARP expression on Tregs but not on tumoral MKs or platelets. Given their known pathogenic role in PMF, MKs were considered to be the most likely source of pathogenic TGF-β1 in this disease.[10,42-44] Our data however, comparing Treg- and MK/platelet-specific *Garp* KO mice, suggest that TGF-β1 presented and activated by GARP on the Treg surface plays a more important role than MK/platelet-derived TGF-β1 in PMF. Tregs are potent suppressors of adaptive immunity and are known to exert detrimental immunosuppression in patients with solid cancer.[45,46] Immunosuppression by Tregs is mediated, at least in part, by the ability of Treg-derived TGF-β1 to inhibit the effector functions of CD8 T cells, which include IFNγ production and cytolysis. Strikingly, we observed that the therapeutic activity of anti-GARP:TGF-β1 in PMF was accompanied by increased IFNγ signals and was lost upon CD8 T-cell depletion. Thus, in addition to limiting the clonal expansion of transformed cells, blocking TGF-β1 activation could reduce immunosuppression by Tregs, thereby increasing the activity of CD8 T cells directed against transformed cells in PMF. Whether T lymphocytes can recognize and kill transformed cells in murine or human PMF has not been formally established. Several HLA class I binding peptides derived from mutated human CALR and MPL proteins have been identified.[47] T cells directed against mutated CALR have been detected in the blood of patients with PMF carrying a CALR mutation.[48-50] Even though improved survival upon PD-1 blockade in murine MPNs suggests the existence of an antitumor T cell activity,[51] this therapy has failed to show evidence of antitumor efficacy in early phase clinical trials.[52,53] However, the absence of response to the immune checkpoint blockade cannot be interpreted as an absence of antitumor T-cell immunity.[47] Whether Tregs suppress the activity of the putative antitumor T cells is not known. Our results suggest that it could be the case, at least in murine PMF.

Figure 5 (continued) fold-change between day 20 and 13 in nontreated controls. Black bars: ES in transcripts ordered by mean fold-change between 58A2 responders and non-treated controls. Green bars: FDR obtained by calculating ES for 1000-gene-set permutations. Right panel shows representative GSEA plots, with black vertical bars indicating position of genes from various gene sets in the ordered transcript list for the responder vs control comparison. EMT, epithelial mesenchymal transition. (C) Heatmap representation of the expression of genes in the leading edge of the IFNγ response signature. Each row represents a gene and each column a mouse. Black boxes on the right indicate genes that are also present in IFNα response signature. (D) Correlation between expression of IFN-induced genes by RNAseq analysis and number of MPL^W508A/GFP+ WBCs in all mice.

Therapeutic approaches to block TGF-β signals in patients with cancer are in clinical development.[54] Current drug candidates include anti–TGF-β antibodies, inhibitors of TGF-β receptor kinase, TGF-β antagonists, and decoy TGF-β receptor constructs. Until now, only limited antitumor effects were observed, together with sometimes severe adverse events, consistent with the importance and diversity of the biological effects mediated by TGF-β. The toxicity of anti–TGF-β drugs has resulted in the early termination of early phase clinical trials, and thus has limited the assessment of their antitumor efficacy. Interestingly, early clinical trials evaluating TGF-β blockade in MF have shown encouraging signs of activity against the disease, with acceptable side effects. One of 2 patients with MF who received repeated administrations of fresolimumab, an mAb that neutralizes the activity of TGF-β1, β2, and β3, achieved anemia improvement and transfusion independence.[55] AVID200, a similar drug that neutralizes TGF-β1 and β3, showed reduced serum levels of its target cytokines and frequent increases in platelet levels.[56] These 2 observations support the active role of TGF-β in PMF-associated anemia and thrombocytopenia and validate the TGF-β signaling pathway as a meaningful therapeutic target in this disease. Anti-GARP:TGF-β1 mAbs, by selectively blocking TGF-β1 production from GARP-expressing cells, such as Tregs, could represent a less toxic alternative. One such antibody is currently being tested as monotherapy or in combination with anti–PD-1 in patients with locally advanced or metastatic solid tumors (ClinicalTrials.gov: NCT03821935).

Our present observations support the clinical evaluation of anti-GARP:TGF-β1 antibodies in patients with MF. Here also, their association with other immunotherapy approaches, and particularly with PD-1/PD–L1 blockade, seems attractive. Combination with other drugs active against myeloproliferative diseases, such as JAK inhibitors, should be handled with caution because the latter drugs may exert suppressive effects on both T-cell activation and antigen presentation.

Authorship

Contribution: S. Lecomte, J.D., D.S., N.V., N.D., and C.P. performed animal, molecular, and cellular biology experiments; S. Lecomte, G.d.S., N.v.B., C. Vanhaver, and C. Vanderaa performed bioinformatics analyses; S. Lecomte, J.D., V.H., S.N.C., and S. Lucas conceived the study; and S. Lecomte, J.D., V.H., N.v.B., P.G.C., S.N.C., and S. Lucas analyzed results and wrote the manuscript.

Conflict-of-interest disclosure: Patents pertaining to blocking antibodies against human GARP:TGF-β1 have been filed under the Patent Cooperation Treaty (International application Number PCT/IB2019/053753) with S. Lucas and P.G.C. as inventors and UCLouvain as applicant. The anti–mouse GARP:TGF-β1 antibody (clone 58A2) used herein is a surrogate for these antibodies. The laboratory of S. Lucas received research funding from AbbVie which licensed the anti-human GARP:TGF-β1 antibodies. The remaining authors declare no competing financial interests.

ORCID profiles: J.D., 0000-0003-0498-5903; G.d.S., 0000-0003-2262-9670; N.v.B., 0000-0003-4548-0266; D.S., 0000-0001-9588-0415; C. Vanderaa, 0000-0001-7443-5427; C.P., 0000-0002-8623-3483; S.N.C., 0000-0002-8599-2699; S. Lucas, 0000-0003-1287-7996.

Correspondence: Sophie Lucas, de Duve Institute, UCLouvain, Ave Hippocrate 74, B1.74.04, B-1200 Brussels, Belgium; email: sophie.lucas@uclouvain.be.

REFERENCES

1. Szuber N, Mudireddy M, Nicolosi M, et al. 3023 Mayo Clinic patients with myeloproliferative neoplasms: risk-stratified comparison of survival and outcomes data among disease subgroups. *Mayo Clin Proc*. 2019;94(4):599-610.

2. Cahu X, Constantinescu SN. Oncogenic drivers in myeloproliferative neoplasms: from JAK2 to calreticulin mutations. *Curr Hematol Malig Rep*. 2015;10(4):335-343.

3. Deininger M, Radich J, Burn TC, Huber R, Paranagama D, Verstovsek S. The effect of long-term ruxolitinib treatment on JAK2p. V617F allele burden in patients with myelofibrosis. *Blood*. 2015;126(13):1551-1554.

4. Harrison C, Kiladjian JJ, Al-Ali HK, et al. JAK inhibition with ruxolitinib versus best available therapy for myelofibrosis. *N Engl J Med*. 2012;366(9):787-798.

5. Vannucchi AM, Kantarjian HM, Kiladjian JJ, et al. A pooled analysis of overall survival in COMFORT-I and COMFORT-II, 2 randomized phase III trials of ruxolitinib for the treatment of myelofibrosis. *Haematologica*. 2015;100(9):1139-1145.

6. Verstovsek S, Mesa RA, Gotlib J, et al. A double-blind, placebo-controlled trial of ruxolitinib for myelofibrosis. *N Engl J Med*. 2012;366(9):799-807.

7. Ballen KK, Shrestha S, Sobocinski KA, et al. Outcome of transplantation for myelofibrosis. *Biol Blood Marrow Transplant*. 2010;16(3):358-367.

8. Chagraoui H, Komura E, Tulliez M, Giraudier S, Vainchenker W, Wendling F. Prominent role of TGF-beta 1 in thrombopoietin-induced myelofibrosis in mice. *Blood*. 2002;100(10):3495-3503.

9. Gastinne T, Vigant F, Lavenu-Bombled C, et al. Adenoviral-mediated TGF-β1 inhibition in a mouse model of myelofibrosis inhibit bone marrow fibrosis development. *Exp Hematol*. 2007;35(1):64-74.

10. Zingariello M, Martelli F, Ciaffoni F, et al. Characterization of the TGF-beta1 signaling abnormalities in the Gata1low mouse model of myelofibrosis. *Blood*. 2013;121(17): 3345-3363.

11. Yue L, Bartenstein M, Zhao W, et al. Efficacy of ALK5 inhibition in myelofibrosis. *JCI Insight*. 2017;2(7):e90932.

12. Stockis J, Colau D, Coulie PG, Lucas S. Membrane protein GARP is a receptor for latent TGF-beta on the surface of activated human Treg. *Eur J Immunol*. 2009;39(12): 3315-3322.

13. Stockis J, Fink W, Francois V, et al. Comparison of stable human Treg and Th clones by transcriptional profiling. *Eur J Immunol*. 2009;39(3):869-882.

14. Stockis J, Lienart S, Colau D, et al. Blocking immunosuppression by human Tregs in vivo with antibodies targeting integrin alphaVbeta8. *Proc Natl Acad Sci U S A*. 2017; 114(47):E10161-E10168.

15. Cuende J, Lienart S, Dedobbeleer O, et al. Monoclonal antibodies against GARP/TGF-beta1 complexes inhibit the immunosuppressive activity of human regulatory T cells in vivo. *Sci Transl Med*. 2015;7(284):284ra256.

16. Lienart S, Merceron R, Vanderaa C, et al. Structural basis of latent TGF-beta1 presentation and activation by GARP on human regulatory T cells. *Science*. 2018; 362(6417):952-956.

17. de Streel G, Bertrand C, Chalon N, et al. Selective inhibition of TGF-beta1 produced by GARP-expressing Tregs overcomes resistance to PD-1/PD-L1 blockade in cancer. *Nat Commun*. 2020;11(1):4545.

18. Rachidi S, Metelli A, Riesenberg B, et al. Platelets subvert T cell immunity against cancer via GARP-TGFbeta axis. *Sci Immunol*. 2017;2(11):eaai7911.

19. Dedobbeleer O, Stockis J, van der Woning B, Coulie PG, Lucas S. Cutting edge: active TGF-beta1 released from GARP/TGF-beta1 complexes on the surface of stimulated human B lymphocytes increases class-switch recombination and production of IgA. *J Immunol*. 2017;199(2):391-396.

20. Metelli A, Wu BX, Riesenberg B, et al. Thrombin contributes to cancer immune evasion via proteolysis of platelet-bound GARP to activate LTGF-beta. *Sci Transl Med*. 2020;12(525);eaay4860.

21. Love MI, Huber W, Anders S. Moderated estimation of fold change and dispersion for RNA-seq data with DESeq2. *Genome Biol*. 2014;15(12):550.

22. Subramanian A, Tamayo P, Mootha VK, et al. Gene set enrichment analysis: a knowledge-based approach for interpreting genome-wide expression profiles. *Proc Natl Acad Sci U S A*. 2005;102(43):15545-15550.

23. Liberzon A, Birger C, Thorvaldsdottir H, Ghandi M, Mesirov JP, Tamayo P. The Molecular Signatures Database (MSigDB) hallmark gene set collection. *Cell Syst*. 2015; 1(6):417-425.

24. Franzen O, Gan LM, Bjorkegren JLM. PanglaoDB: a web server for exploration of mouse and human single-cell RNA sequencing data. *Database*. 2019;2019:1-9.

25. Decker M, Martinez-Morentin L, Wang G, et al. Leptin-receptor-expressing bone marrow stromal cells are myofibroblasts in primary myelofibrosis. *Nat Cell Biol*. 2017; 19(6):677-688.

26. Pikman Y, Lee BH, Mercher T, et al. MPLW515L is a novel somatic activating mutation in myelofibrosis with myeloid metaplasia. *PLoS Med*. 2006;3(7):e270.

27. Pecquet C, Staerk J, Chaligne R, et al. Induction of myeloproliferative disorder and myelofibrosis by thrombopoietin receptor W515 mutants is mediated by cytosolic tyrosine 112 of the receptor. *Blood*. 2010; 115(5):1037-1048.

28. Kuter DJ, Bain B, Mufti G, Bagg A, Hasserjian RP. Bone marrow fibrosis: pathophysiology and clinical significance of increased bone marrow stromal fibres. *Br J Haematol*. 2007;139(3):351-362.

29. Varricchio L, Iancu-Rubin C, Upadhyaya B, et al. TGF-beta1 protein trap AVID200 beneficially affects hematopoiesis and bone marrow fibrosis in myelofibrosis. *JCI Insight*. 2021;6(18):e145651.

30. Ceglia I, Dueck AC, Masiello F, et al. Preclinical rationale for TGF-beta inhibition as a therapeutic target for the treatment of myelofibrosis. *Exp Hematol*. 2016;44(12): 1138-1155.e1134.

31. Yao J-C, Link DC. TGF-β signaling contributes to the clonal dominance of Jak2V617F hematopoietic stem/progenitor cells [abstract]. *Blood*. 2020;136(suppl 1). Abstract 718.

32. Komatsu N, Hori S. Full restoration of peripheral Foxp3+ regulatory T cell pool by radioresistant host cells in scurfy bone marrow chimeras. *Proc Natl Acad Sci U S A*. 2007;104(21):8959-8964.

33. Wen QJ, Yang Q, Goldenson B, et al. Targeting megakaryocytic-induced fibrosis in myeloproliferative neoplasms by AURKA inhibition. *Nat Med*. 2015;21(12):1473-1480.

34. Woods B, Chen W, Chiu S, et al. Activation of JAK/STAT signaling in megakaryocytes sustains myeloproliferation in vivo. *Clin Cancer Res*. 2019;25(19):5901-5912.

35. Kleppe M, Kwak M, Koppikar P, et al. JAK-STAT pathway activation in malignant and nonmalignant cells contributes to MPN pathogenesis and therapeutic response. *Cancer Discov*. 2015;5(3):316-331.

36. Chambers RC, Leoni P, Kaminski N, Laurent GJ, Heller RA. Global expression profiling of fibroblast responses to transforming growth factor-beta1 reveals the induction of inhibitor of differentiation-1 and provides evidence of smooth muscle cell phenotypic switching. *Am J Pathol*. 2003; 162(2):533-546.

37. Hasan S, Lacout C, Marty C, et al. JAK2V617F expression in mice amplifies early hematopoietic cells and gives them a competitive advantage that is hampered by IFNalpha. *Blood*. 2013;122(8):1464-1477.

38. Yamazaki S, Ema H, Karlsson G, et al. Nonmyelinating Schwann cells maintain hematopoietic stem cell hibernation in the bone marrow niche. *Cell*. 2011;147(5):1146-1158.

39. Brenet F, Kermani P, Spektor R, Rafii S, Scandura JM. TGFbeta restores hematopoietic homeostasis after myelosuppressive chemotherapy. *J Exp Med*. 2013;210(3):623-639.

40. Zhao M, Perry JM, Marshall H, et al. Megakaryocytes maintain homeostatic quiescence and promote post-injury regeneration of hematopoietic stem cells. *Nat Med*. 2014;20(11):1321-1326.

41. Jiang L, Han X, Wang J, et al. SHP-1 regulates hematopoietic stem cell quiescence by coordinating TGF-beta signaling. *J Exp Med*. 2018;215(5):1337-1347.

42. Bock O, Loch G, Schade U, von Wasielewski R, Schlue J, Kreipe H. Aberrant expression of transforming growth factor beta-1 (TGF beta-1) per se does not discriminate fibrotic from non-fibrotic chronic myeloproliferative disorders. *J Pathol*. 2005; 205(5):548-557.

43. Ponce CC, de Lourdes FCM, Ihara SS, Silva MR. The relationship of the active and latent forms of TGF-beta1 with marrow fibrosis in essential thrombocythemia and primary myelofibrosis. *Med Oncol*. 2012;29(4):2337-2344.

44. Ciurea SO, Merchant D, Mahmud N, et al. Pivotal contributions of megakaryocytes to the biology of idiopathic myelofibrosis. *Blood*. 2007;110(3):986-993.

45. Tanaka A, Sakaguchi S. Regulatory T cells in cancer immunotherapy. *Cell Res*. 2017;27(1): 109-118.

46. Sakaguchi S, Mikami N, Wing JB, Tanaka A, Ichiyama K, Ohkura N. Regulatory T cells, and human disease. *Annu Rev Immunol*. 2020;38: 541-566.

47. Schischlik F, Jager R, Rosebrock F, et al. Mutational landscape of the transcriptome offers putative targets for immunotherapy of myeloproliferative neoplasms. *Blood*. 2019; 134(2):199-210.

48. Holmstrom MO, Riley CH, Svane IM, Hasselbalch HC, Andersen MH. The CALR exon 9 mutations are shared neoantigens in patients with CALR mutant chronic myeloproliferative neoplasms. *Leukemia*. 2016;30(12):2413-2416.

49. Holmstrom MO, Martinenaite E, Ahmad SM, et al. The calreticulin (CALR) exon 9 mutations

are promising targets for cancer immune therapy. *Leukemia.* 2018;32(2):429-437.

50. Cimen Bozkus C, Roudko V, Finnigan JP, et al. Immune checkpoint blockade enhances shared neoantigen-induced T-cell immunity directed against mutated calreticulin in myeloproliferative neoplasms. *Cancer Discov.* 2019;9(9):1192-1207.

51. Prestipino A, Emhardt AJ, Aumann K, et al. Oncogenic JAK2(V617F) causes PD-L1 expression, mediating immune escape in myeloproliferative neoplasms. *Sci Transl Med.* 2018;10(429).

52. Abou Dalle I, Kantarjian H, Daver N, et al. Phase II study of single-agent nivolumab in patients with myelofibrosis. *Ann Hematol.* 2021;100(12):2957-2960.

53. Hobbs G, Cimen Bozkus C, Moshier E, et al. PD-1 inhibition in advanced myeloproliferative neoplasms. *Blood Adv.* 2021;5(23):5086-5097.

54. Teicher BA. TGFbeta-directed therapeutics: 2020. *Pharmacol Ther.* 2021;217:107666.

55. Mascarenhas J, Li T, Sandy L, et al. Anti-transforming growth factor-beta therapy in patients with myelofibrosis. *Leuk Lymphoma.* 2014;55(2):450-452.

56. Mascarenhas J, Kosiorek HE, Bhave R, et al. Treatment of myelofibrosis patients with the TGF-β 1/3 Inhibitor AVID200 (MPN-RC 118) induces a profound effect on platelet production [abstract]. *Blood.* 2021;138(suppl 1). Abstract 142.

LECOMTE et al